Mass Transfer between Solid and Liquid in a Gas-Stirred Vessel

AMARENDRA K. SINGH and DIPAK MAZUMDAR

Mass transfer between solid and bulk liquid in an axisymmetric gas-stirred water model of a metallurgical reactor has been investigated both experimentally and theoretically. To this end, mass transfer rates from benzoic acid compacts submerged in an aqueous gas bubble driven system were measured *via* a weight loss technique. In conjunction with the weight loss measurements, liquid velocity and turbulence kinetic energy distributions in the bath were also mapped *via* laser doppler velocimetry (LDV). From the detailed LDV measurements, relevant dimensionless groups such as $\mathrm{Re}_{\mathrm{loc},r}\left(=\frac{d\rho\sqrt{u^2+v^2}}{\mu}\right)$ and $\mathrm{Re}_t\left(=\frac{d\rho\hat{u}}{\mu}\right)$ were estimated. Experimental measurements indicated that flow parameters varied from one location to another within the system. The corresponding variation in dissolution rates was, however, less pronounced. Such a trend was observed for all three gas flow rates studied. It was found that experimentally measured dissolution rates can be correlated with the measured flow and turbulence parameters (*viz.*, $\sqrt{u^2+v^2}$ and $\hat{u}$) in terms of a previously reported dimensionless correlation, viz., $\mathrm{Sh} = 0.73\ (\mathrm{Re}_{\mathrm{loc},r})^{0.25}\ (\mathrm{Re}_t)^{0.32}\ (\mathrm{Sc})^{0.33}$. Parallel to flow measurements, a two-phase turbulent flow model was also applied to numerically compute the distributions of mean and fluctuating velocity components in the vessel. Embodying the predicted velocity components in the aforementioned correlation, mass transfer rates were recalculated. A comparison between the two sets of Sherwood numbers (estimated on the basis of the experimentally measured and theoretically predicted flow fields) suggests that solid-liquid mass transfer rates in a gas-stirred vessel can be predicted reasonably well *via* an axisymmetric, steady-state, two-dimensional turbulent flow model.

I. INTRODUCTION

MASS transfer between solid and liquid is an essential and integral feature of many pyrometallurgical operations carried out in metallurgical furnaces, ladles, *etc.* As examples of this, processes such as alloying and powder injection can be readily visualized. The large size of metallurgical reactors (*i.e.*, today's refining and holding vessels often contain as much as 500 tonnes of hot metal) coupled with the high intensity of agitation (*e.g.*, large specific gas flows associated with near sonic velocities are often applied to stir melts) often preclude low Reynolds number flows in metal processing units. Thus, many investigations carried out so far[1–8] have indicated that in typical material processing operations, the intensity of turbulence is very often appreciable, and therefore, classical correlations for translatory flows are insufficient to realistically connect the hydrodynamic phenomena to transport rates. This, reproduced from the work of Taniguchi *et al.*,[2] is illustrated in Figure 1. There, the classical Ranz–Marshall correlation[9] is seen to underestimate heat transfer rates of ice spheres in an aqueous gas bubble driven system by about 40 to 50 pct. Consequently, to simulate the melting phenomena realistically, Taniguchi *et al.*[2] considered a modified version of the Ranz–Marshall correlation applicable to the turbulent flow situation.[6]

In turbulent metal processing operations, the combined influence of flow and turbulence on heat and mass transfer is generally well recognized, and accordingly, several new transport correlations have been proposed in recent years. A summary of these is presented in Table I. In developing or adapting[1,2,8] these correlations to infer melting and/or dissolution rates, practically in all the studies[1,4,8] reported to date, theoretically estimated velocity and turbulence kinetic energy fields were embodied in the various dimensionless groups, *viz.*, $\mathrm{Re}_{\mathrm{loc},r}$, Re_t, Tu, *etc.* (the List of Symbols provides explanation). To this end, while Szekely *et al.*[3] as well as Mazumdar *et al.*[4] applied a computational procedure based on the numerical solution of turbulent Navier–Stokes equations, Taniguchi *et al.*[2] and Koria[8] applied a macroscopic energy balance. No attempt has yet been made to assess the predictive capabilities of these correlations with reference to experimentally determined flow and turbulence kinetic energy fields. This is of concern since numerical simulation of flow phenomena is known to provide only approximate distributions of the turbulence characteristics (k, ε, μ_t, *etc.*) in gas bubble driven systems.[10,11,12]

The purpose of the present work, consequently, has been to assess the adequacy and appropriateness of the various Sherwood number based correlations presented in Table I,[1,4,8] applied so far to investigate metal processing operations, from a purely experimental standpoint. To this end, experimental observations on the dissolution rates of solid benzoic acid compacts and the associated flow fields (both mean and turbulent) in an aqueous gas bubble driven system ($L = 0.21$ m and $D = 0.30$ m) are presented in subsequent sections. In conjunction with these, a steady-state, two-phase, turbulent flow calculation procedure[13] has also

AMARENDRA K. SINGH, Scientist, is with the Tata Research, Development and Design Centre, Pune, Maharashtra, 411001 India. DIPAK MAZUMDAR, Professor, is with the Department of Materials and Metallurgical Engineering, Indian Institute of Technology, Kanpur, UP, 208016 India.

Manuscript submitted December 20, 1995.

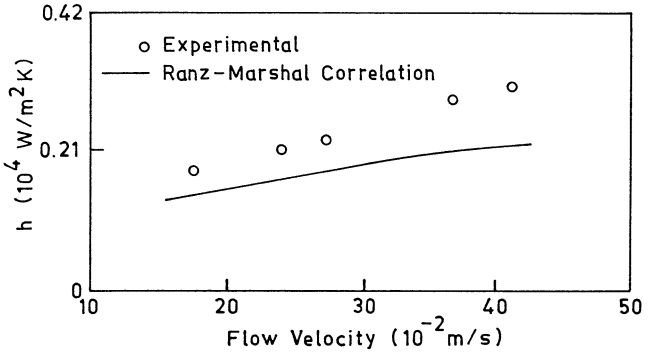

Fig. 1—Experimentally measured heat transfer coefficients and their comparison with those predicted *via* the Ranz–Marshall correlation, $Nu = 2 + 0.6Re^{1/2}Pr^{1/3}$, in a gas bubble driven system (reproduced from the work of Taniguchi *et al.*[2]).

been applied to primarily re-examine the validity of the approach currently being followed,[1–4,8] toward estimation of heat and/or mass transfer rates in metallurgical systems.

II. EXPERIMENTAL WORK

A. *Measurements of Dissolution Rates*

The experimental setup used in the present study consisted of a cylindrical tank containing water and agitated by a stream of air introduced through a submerged vertical lance located centrally within the vessel. A copper tube, having an inner diameter of 3 mm, was used as the lance. The tip of the lance was located at a height of about 10 mm from the base of the model vessel. Four benzoic acid cylinders attached to a supporting assembly were introduced vertically (*viz.* the axes of the acid compacts being kept parallel to the axis of the vessel) at various locations inside the agitated mass of water, as illustrated schematically in Figure 2. The rates of dissolution of these cylindrical compacts were monitored by the weight loss method. To this end, the acid compacts were periodically taken out from the bath, dried, and their weights recorded.

Figure 2 is a schematic of the apparatus used, which also shows the position of the four samples in the bulk aqueous phase. Both ends of the cylindrical compacts were sealed so as to ensure only radial mass transfer. These cylinders were prepared in the laboratory by melting and casting of commercial grade benzoic acid using metallic molds.

At the beginning of each experiment, gas flow was started and sufficient time allowed for the attainment of steady-state flow conditions. Subsequent to this, the samples attached to the supporting assembly were introduced into water. At intervals of 600 seconds, the assembly was taken out from the bath, the samples detached, and their weights recorded by a digital balance after thorough drying. Three different gas flow rates were studied, and at each flow rate, at least three sets of measurements on weight loss were made at each location. Reproducibility of measurements was within ± 10 pct.

B. *Measurements of Mean Flow and Turbulence Characteristics of the Gas-Stirred Bath*

Steady-state velocity fields (*e.g.*, the mean components of fluid motion) together with their associated level of fluctuations (*viz.*, turbulence velocity) were measured in the aqueous phase contained within the cylindrical PLEXIGLASS* tank as a function of the three different gas flow rates applied. To this end, laser doppler velocimetry (LDV) was used. The LDV setup assembled in this study was a backscatter type employing a 15-mW helium-neon laser. Bursts of laser light, scattered from impurity particles (10-μm silicon carbide) added to the flowing water, were collected by the photo detector. This converted the optical signals for processing by a 1990A type counter supplied by TSI. The processed signals were subsequently analyzed with a microcomputer. Time average and fluctuating components of the flow (*i.e.*, $\overline{u}$, $\overline{v}$, u', and v') at each gas flow rate were measured at eight different axial positions and at six different radial positions for a total of 48 different locations. At each location, approximately 1000 data points were collected at a mean rate of about 50 per second. The lower limit of detection with the LDV assembled was 1 cm/s. The maximum variation observed in mean velocity components for successive measurements at a given location was 0 to 2 cm s^{-1}. On the basis of these, the axial and the radial velocity components together with the corresponding velocity fluctuations prevalent in the immediate vicinity of the submerged acid compacts were obtained. To ensure steady-state conditions, velocity measurements were taken, after allowing the gas to flow for 10 minutes into the quiescent vessel.

*PLEXIGLASS is a trademark of Rohm & Haas Company, Philadelphia, PA.

III. RESULTS AND DISCUSSION

In interpreting the results of the weight loss experiments, the instantaneous weight values for each sample were first reduced to corresponding equivalent average radius values (*e.g.*, $\pi\rho_s L[R^2 - R_i^2] = \Delta m$). As a sample illustration, the variation of average instantaneous radius as a function of dissolution time for all four samples at a gas flow rate of 3.3×10^{-5} m^3/s is shown in Figure 3. This clearly shows that the weight loss data can be correlated with reasonable certainty by means of straight lines passing through the experimental data points. Furthermore, the projected intercepts on the ordinate at $t = 0$ s for each line were found to be sufficiently close to the initial sample radii values, indicating essentially that the mass transfer took place under steady-state flow conditions.

Figure 3 also contains the values of slope ($-dR/dt$) for all four straight lines. There, the dissolution rates (proportional to $-dR/dt$) are seen to be spatially dependent. This is to be expected, since bulk liquid flows and turbulence characteristics, which determine the rate of dissolution, also vary from one location to another in the system (as subsequently discussed). It is instructive to note here that flow and turbulence parameters in gas-stirred systems vary appreciably, being intense in the plume and free-surface regions and sluggish in the vicinity of bottom walls/corners of the vessel.[14,15]

To represent the experimental data on slope, $-dR/dt$, as a function of various locations and gas flow rates in a comprehensive fashion, these were first reduced to equivalent, average mass transfer coefficient values according to

Table I. A Summary of Various Correlations Applied to Investigate Heat and Mass Transfer Phenomena in Metal Processing Operations

Solution Number	Reference	Correlations	Remarks
1	Szekely *et al.*[1]	$Sh = 2 + 0.7Re^{0.5}Re_t^{0.25}Sc^{0.33}$	adapted from literature: originally developed by Lavender and Pei[5] for spherical geometry in turbulent shear flows
2	Taniguchi *et al.*[2]	$(Nu - 2) = [0.4Re^{0.5} + 0.06Re^{0.66}] Pr^{0.4} (\mu_b/\mu_0)^{0.25}$	adapted from literature: originally developed by Whitaker[6] for spherical geometry
3	Szekely *et al.*[3]	$Nu = 0.8(ReTu)^{0.8} Pr^{0.33}$	developed for analysis of melting phenomena in turbulent gas stirred reactors
4	Mazumdar *et al.*[4]	$Sh = 0.73Re^{0.25} Re_t^{0.32} Sc^{0.33}$	developed for analysis of dissolution phenomena in turbulent gas stirred reactors
5	Koria[8]	$Sh = 0.79Re^{0.7} Sc^{0.356}$	recommended by Asai et al.[7] for analysis of dissolution phenomena in ladle metallurgy steelmaking operations

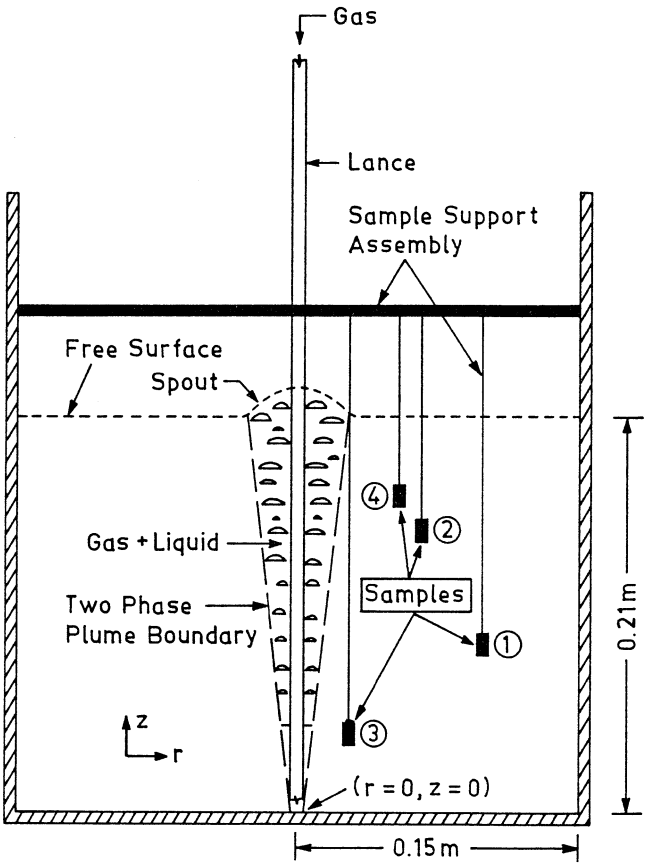

Fig. 2—Schematic of the experimental apparatus used in the present investigation.

$$-\frac{dM}{dt} = K_{av}A(C_s^* - C_b) \qquad [1]$$

Furthermore, considering $M = \rho_s \pi R^2 L$ and $A = 2\pi RL$ and setting $C_b = 0$, the average mass transfer coefficient, K_{av}, in Eq. [1], can be represented as

$$K_{av} = -(dR/dt)\ \rho_s/C_s^* \qquad [2]$$

Equation [1] is a statement of mass balance derived on the basis of the assumption that mass transfer across the concentration boundary layer is the rate limiting step. In addition to this, the bulk concentration of benzoic acid in water, C_b in Eq. [2], has been assumed to be zero. In applying Eq. [1] to the present analysis, it has been tacitly assumed that the hydrodynamic erosion as well as drying of the benzoic acid samples does not contribute to mass loss and, hence, the observed mass transfer rates. Average mass transfer coefficients thus estimated have been summarized in Table II, together with the corresponding values of the Sherwood number ($=K_{av}d/D_0$). Similarly, in Table III, the values of relevant thermophysical properties and other data employed in the present investigation are shown. It is important to mention here that the individual slope ($-dR/dt$) value, shown in Table II, is an average value, estimated from three different sets of measurements, while those in Figure 3 are the values obtained from a particular experiment.

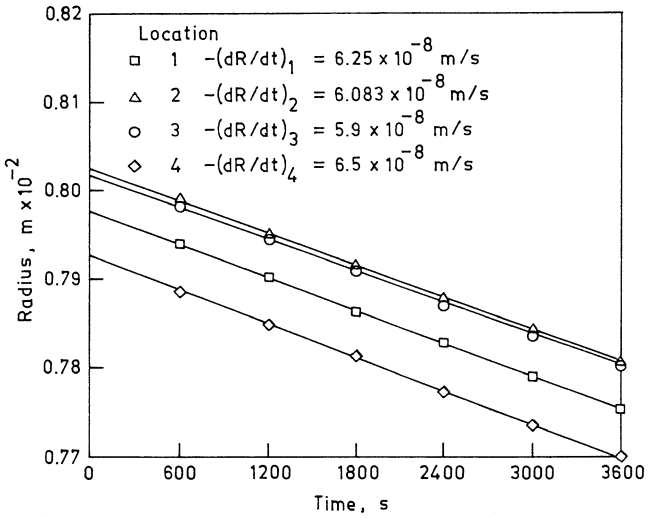

Fig. 3—Experimentally measured dissolution rates ($\propto -dR/dt$) at four different locations in the bath at a gas flow rate of 0.33×10^{-4} m³/s.

Figures 4(a) and (b), respectively, show a typical map of measured time-averaged and corresponding fluctuating velocity components in the gas-stirred vessel at a gas flow of 0.33×10^{-4} m³/s. There, the numbers within the parentheses indicate, respectively, the axial and the radial direction velocity components. These figures also contain the locations in the bath at which the benzoic acid cylindrical com-

Table II. Summary of Experimental Measurements on Average Mass Transfer Coefficients and Corresponding Sherwood Number for Various Locations as a Function of Gas Flow Rate

Gas Flow Rate (m^3/s)	Initial Sample Radius (10^{-2} m)	Location	Slope ($-dR/dt$) (10^{-2} m/s)	Average Mass Transfer Coefficient (10^{-2} m/s)	Sherwood Number ($K_{av}d/D_0$)
1.66×10^{-5}	0.8486	1	5.665×10^{-6}	1.72×10^{-3}	145
	0.7903	2	5.950×10^{-6}	1.81×10^{-3}	143
	0.8052	3	5.450×10^{-6}	1.65×10^{-3}	133
	0.7445	4	5.730×10^{-6}	1.74×10^{-3}	130
3.33×10^{-5}	0.8184	1	6.120×10^{-6}	1.86×10^{-3}	152
	0.8031	2	6.410×10^{-6}	1.95×10^{-3}	156
	0.8067	3	6.130×10^{-6}	1.86×10^{-3}	150
	0.7824	4	6.290×10^{-6}	1.91×10^{-3}	150
5.00×10^{-5}	0.8087	1	6.290×10^{-6}	1.91×10^{-3}	154
	0.8140	2	7.240×10^{-6}	2.20×10^{-3}	179
	0.8119	3	6.630×10^{-6}	2.01×10^{-3}	164
	0.8117	4	6.870×10^{-6}	2.09×10^{-3}	170

pacts were kept immersed. Since the samples were placed in the bulk single-phase region, LDV measurements were consequently restricted in the single-phase region. No attempt was made to measure liquid velocity components in the two-phase, gas-liquid region. On the basis of LDV measurements (Figure 4(a)), the resultant mean velocity components, $\sqrt{u^2 + v^2}$, prevalent at locations around the submerged solids, were estimated. Similarly, from the measured fluctuating velocity components (Figure 4(b)), the specific turbulence kinetic energy, $k = \frac{1}{2}[u'^2 + v'^2 + w'^2]$, was first estimated at each location considering w' to be equal to v'. On the basis of such, relevant isotropic fluctuating velocity components were subsequently calculated from $\hat{u} = \sqrt{\frac{2}{3}k}$. Resultant velocity components together with the corresponding isotropic fluctuation velocity components thus estimated are summarized in Table IV at four different locations and as a function of three different gas flow rates. It is important to mention here that since the LDV equipment assembled had a minimum velocity detection level of 1 cm s^{-1}, a zero level of turbulence was indicated experimentally at many locations, particularly at the lowest gas flow rate studied ($=0.166 \times 10^{-4}$ m^3/s). At such locations, however, a minimum intensity of turbulence of about 0.21 was assumed,[14] and based on such a consideration, an isotropic fluctuating velocity component equal to $0.21\sqrt{u^2 + v^2}$ was applied for estimating the turbulent Reynolds number. The nominal Reynolds number, $\mathrm{Re}_{\mathrm{loc},r}$ $\left(\frac{d\rho\sqrt{u^2 + v^2}}{\mu}\right)$, and turbulent Reynolds number, Re_t $\left(=\frac{d\rho\hat{u}}{\mu}\right)$, thus estimated have been summarized in Table IV for all 12 different experimental conditions.

With reference to the results presented in Table IV, it is instructive to note here that the flow measurements summarized are those obtained in the absence of submerged solid samples, since the measurements in the aqueous phase were primarily carried out under such conditions. A couple of measurements, however, indicated that at velocity measuring locations (Figure 4(a)), practically identical results were obtained regardless of whether solid samples were present or absent in the aqueous phase. This is to be expected since the volume fraction of submerged solid samples is a small fraction (~2 pct) of the reactor volume. It is important to mention here that any marginal variations, which are likely to occur between the two configurations (no solid *vs*/solid), were perhaps beyond the level of sensitivity of the LDV equipment assembled.

Table III. Values of Thermophysical Properties and Other Relevant Data Employed in the Present Investigation

1.	Density of benzoic acid, kg/m^3	1.26×10^{-3}
2.	Solubility of benzoic acid in water at 26 °C, kg/m^3	4.074
3.	Diffusivity of benzoic acid in water, m^2/s	2.09×10^{-9}
4.	Density of water, kg/m^3	10^3
5.	Viscosity of water, kg/(m·s)	10^{-3}

In Figures 5(a) through (c), the variation of dissolution rates is shown as a function of the Reynolds number in order to assess the present experimental measurements in terms the three different mass transfer correlations[1,4,8] presented in Table I. There, it is readily seen that the correlation reported earlier by Mazumdar *et al.*[4] (*viz.*, $\mathrm{Sh} = 0.73(\mathrm{Re}_{\mathrm{loc},r})^{0.25}(\mathrm{Re}_t)^{0.32}(\mathrm{Sc})^{0.33}$) alone provides estimates of mass transfer rates which are in reasonable agreement with the experimental measurements. In contrast, the correlation[7] $\mathrm{Sh} = 0.079(\mathrm{Re})^{0.7}(\mathrm{Sc})^{0.356}$ is seen to underestimate the dissolution rates considerably. This is to be expected since the correlation[7] does not account for any possible contribution from fluid turbulence to mass transfer rates. Similarly, the correlation $\mathrm{Sh} = 2.0 + 0.7(\mathrm{Re}_{\mathrm{loc},r})^{0.5}(\mathrm{Re}_t)^{0.32}(\mathrm{Sc})^{0.33}$, which was originally developed for mass transfer from spherical objects in turbulent shear flows,[5] is seen to be inadequate for the present purpose.

In their earlier study, as has been pointed out already, Mazumdar *et al.*[4] applied a quasi-single-phase mathematical model to estimate the distribution of flow ($\bar{u}$ and $\bar{v}$) and turbulence ($\hat{u}$) parameters in the gas-stirred bath and embodied these in various dimensionless groups such as $\mathrm{Re}_{\mathrm{loc},r}$ and Re_t. In the numerical calculation procedure,[4] an empirically determined geometry of the two-phase region to-

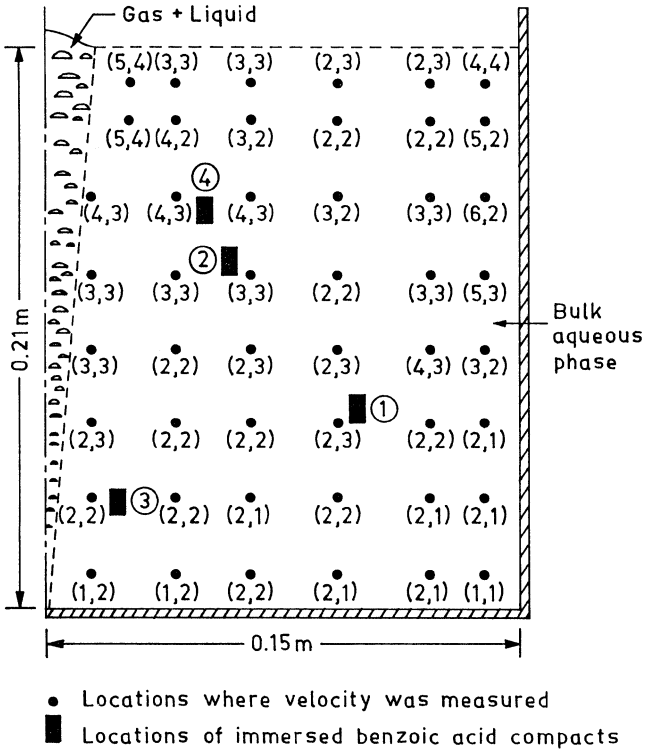

(*a*)

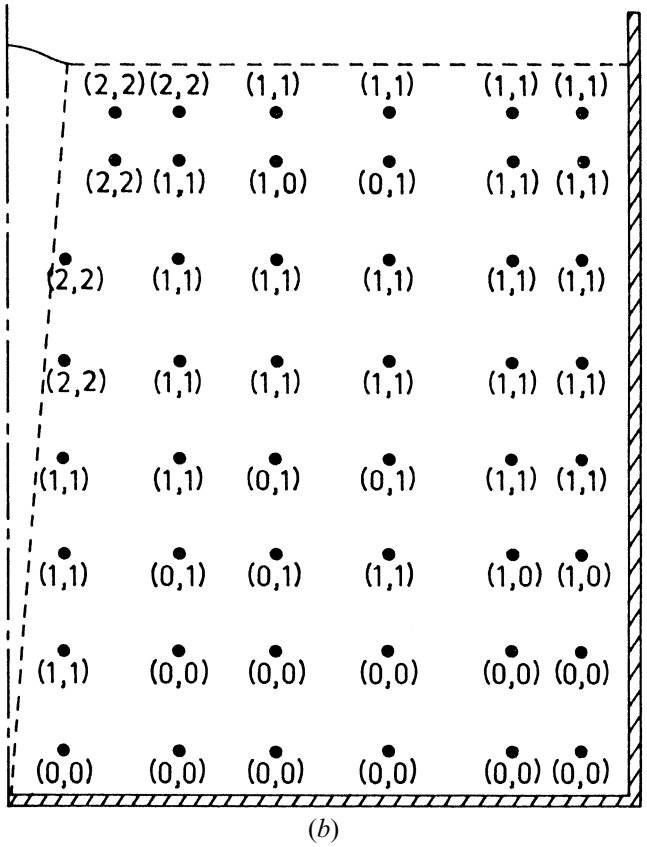

(*b*)

Fig. 4—Experimentally measured velocity fields (in 10^{-2} m/s) in the water model at a gas flow rate of 0.33×10^{-4} m^3/s: (*a*) $|u|$ and $|v|$ components and (*b*) RMS of the velocity fluctuation along the axial and radial directions (u' and v').

gether with an *a priori* estimated gas volume fraction within the bubble plume was applied. Although many previous studies[1,3,4] appear to indicate that quasi-single-phase flow models are adequate and are likely to provide reasonable estimates of the mass transfer rate in gas-stirred systems, an attempt has been made in the present study to test the experimental data reported so far against corresponding predictions from a relatively more rigorous two-phase, turbulent flow model.[13] There,[13] the liquid-phase momentum balance equations were coupled with a bubble trajectory equation and applied in conjunction with the standard coefficient k-ε turbulence model.[17] The turbulence model contained an empirically fitted additional turbulence generation term, to accommodate for the generation of turbulence within the two-phase region, due to bubble-liquid interactions. It is important to note here that only two empirical parameters, *viz.*, the drag coefficient and bubble diameter, were required as initial input to predict the flow phenomena from first principles. Details of the calculation procedure have been reported elsewhere[13] and, therefore, not reproduced here.

Thus, from the theoretically predicted distributions of flow variables ($\bar{u}$ and $\bar{v}$) and turbulence parameters (k, ε, $\hat{u}$, *etc.*) in the vessel, relevant mean and fluctuating velocity components prevalent at locations around the submerged solids were deduced. On the basis of these results, summarized in Table V, corresponding nominal ($Re_{loc,r}$) and turbulent (Re_t) Reynolds numbers were deduced. These were subsequently embodied in the correlation,[4] and all the mass transfer rates (*viz.*, Sh) were estimated. The two sets of estimated Sherwood numbers based on theoretically estimated and experimentally determined velocity fields are shown in Figure 6 vis-à-vis the mass transfer correlation, $Sh = 0.73(Re_{loc,r})^{0.25}(Re_t)^{0.32}(Sc)^{0.33}$. There, despite some differences in the value of the estimated turbulent Reynolds numbers (or $\hat{u}$, as shown in Tables IV and V, respectively), the two-phase, turbulent flow model, in conjunction with the preceding correlation, is seen to produce reasonable estimates of mass transfer rates in the gas bubble driven system. Furthermore, a comparison of experimental and computed results, summarized in Tables IV and V, indicates that while the predicted fluctuating velocity component in the bath has been overestimated to some extent, the corresponding mean flow component has been underestimated. Furthermore, the value of the quantity $(Re_{loc,r})^{0.25}(Re_t)^{0.32}$ was evaluated, which was found to be practically identical to those for the corresponding conditions summarized in Tables IV and V. As a consequence of this, it can be anticipated that the estimated Sherwood numbers for the two situations are also likely to be very similar. It is instructive to note here that the inadequacy of the k-ε turbulence model[17] in simulating turbulence phenomena in the gas-stirred baths is rather well known.[3,11,12] Although attempts have been made[12] to empirically tune the standard coefficient k-ε turbulence model to gas-stirred metallurgical reactors,[12,18] these were, nevertheless, only partially successful. Nonetheless, such inadequacies are of no serious consequence as far as the present study is concerned, since mass transfer rates are a relatively weak function of $\sqrt{u^2 + v^2}$ and $\hat{u}$. The present work, therefore, appears to suggest that the mass transfer correlation,

Table IV. Experimentally Determined Time-Averaged and Fluctuating Velocity Components at Various Locations in the Bath as a Function of Gas Flow Rates

Gas Flow Rate (m^3/s)	Initial Sample Radius (10^{-2} m)	Locations	$\sqrt{u^2 + v^2}$ (10^{-3} m/s)	$\hat{u}$ (10^{-3} m/s)	Reynolds Number $d\rho\sqrt{u^2 + v^2}/\mu$	Turbulent Reynolds Number $(d\rho\hat{u}/\mu)$
	0.8486	1	25.0	5.6	424	95
1.66×10^{-5}	0.7903	2	28.3	8.1	447	128
	0.8052	3	22.4	8.1	361	131
	0.7445	4	36.1	8.1	537	120
	0.8184	1	36.1	9.4	591	154
3.33×10^{-5}	0.8031	2	42.4	10.0	681	161
	0.8067	3	28.3	10.0	456	161
	0.7824	4	50.0	10.0	782	156
	0.8087	1	41.0	10.0	663	162
5.00×10^{-5}	0.8140	2	58.3	10.0	949	163
	0.8119	3	42.4	10.7	688	173
	0.8117	4	50.0	10.0	812	162

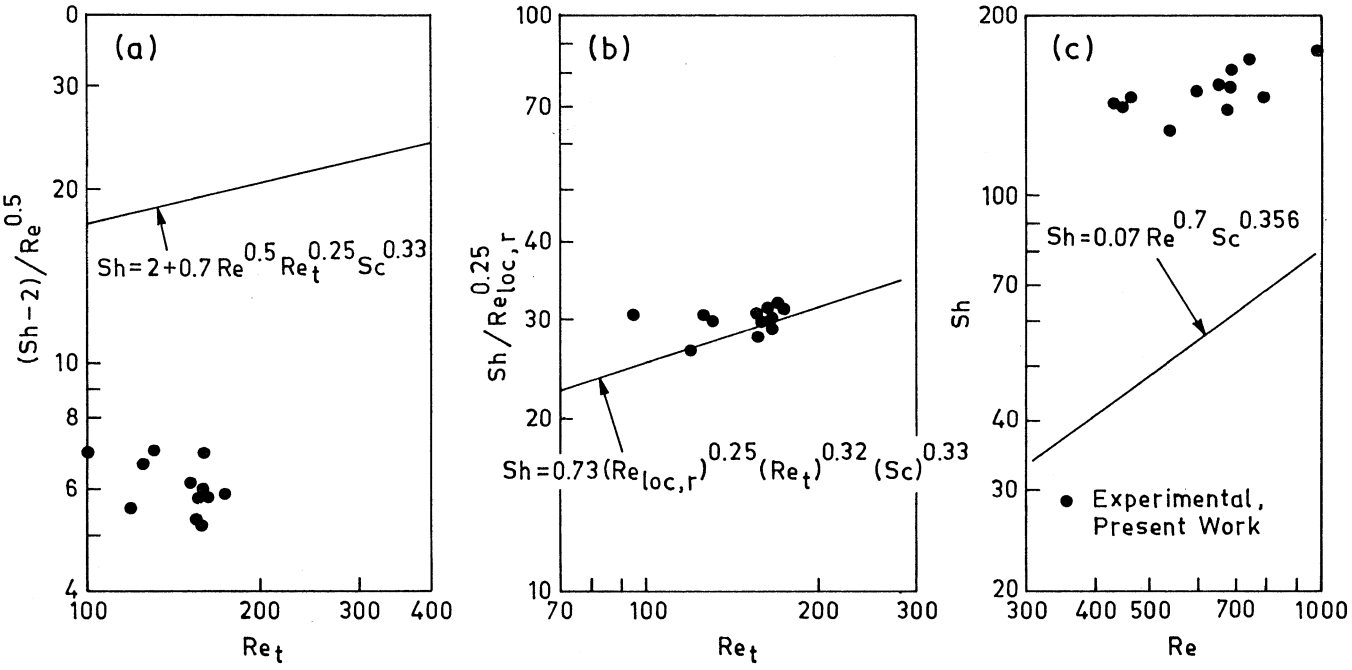

Fig. 5—Comparison of present experimental measurements of dissolution rates *via* the three different correlations reported in the literature[1,4,8] using experimentally determined velocity fields.

$Sh = 0.73(Re_{loc,r})^{0.25}(Re_t)^{0.32}(Sc)^{0.33}$, together with the two-phase turbulent flow model,[16] provides a reasonable starting point for investigating solid-liquid mass transfer rates in complex, difficult to investigate, gas bubble driven metallurgical reactors.

Finally, to assess the predictive capabilities of the present approach beyond its currently validated limits of vessel size, liquid, *etc.*, the model developed in the present study has been extrapolated to investigate isothermal dissolution of steel rods in a 25-kg laboratory scale, axisymmetric gas-stirred Fe-C bath.[19] Since the specific gas flows applied in the experimental work by Wright[19] were similar to those encountered in typical ladle metallurgy steelmaking operations and those considered in the present study, the two-phase hydrodynamic model[16] can be conveniently applied to the experimental conditions of Wright. Thus, assuming a bubble size and a drag coefficient–Reynolds number relationship, the distribution of flow and turbulence parameters in the high-temperature system[19] has been predicted. The vessel containing the 25-kg Fe-C melt was a cylindrical shaped one having a tapered bottom. To simulate the tapered bottom and thus the exact vessel geometry, the computational procedure of Moult *et al.*[20] was adapted into the two-phase flow model. The model was run for five different gas flow rates to numerically estimate the distributions of flow and turbulence quantities in the melt. Incorporating

Table V. Theoretically Predicted Time-Averaged and Fluctuating Velocity Components at Various Locations in the Bath as a Function of Gas Flow Rates

Gas Flow Rate (m^3/s)	Initial Sample Radius (10^{-2} m)	Locations	$\sqrt{u^2 + v^2}$ (10^{-3} m/s)	$\hat{u}$ (10^{-3} m/s)	Reynolds Number $d\rho\sqrt{u^2 + v^2}/\mu$	Turbulent Reynolds Number $(d\rho\hat{u}/\mu)$
	0.8486	1	22	12	373	203
1.66×10^{-5}	0.7903	2	31	19	490	300
	0.8052	3	37	20	596	322
	0.7445	4	10	14	149	209
	0.8184	1	28	18	458	294
3.33×10^{-5}	0.8031	2	38	19	610	305
	0.8067	3	48	23	774	371
	0.7824	4	13	24	203	374
	0.8087	1	28	15	453	243
5.00×10^{-5}	0.8140	2	42	22	684	358
	0.8119	3	46	24	747	390
	0.8117	4	14	30	227	486

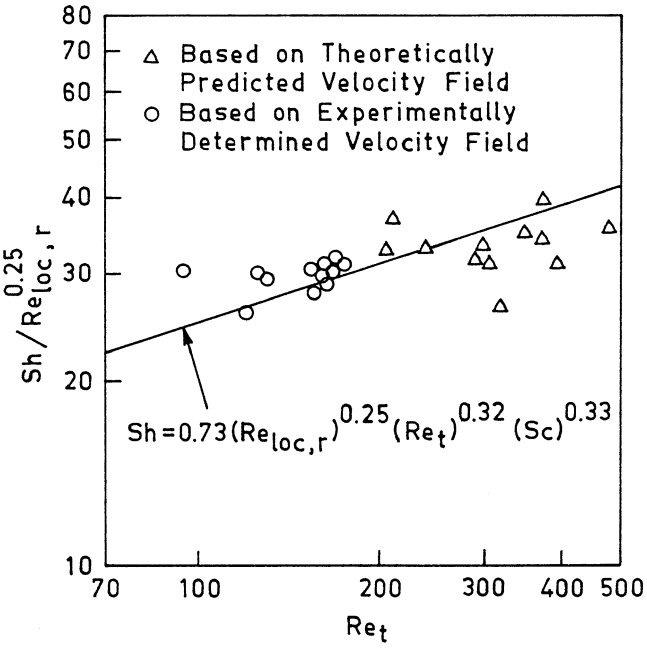

Fig. 6—The correlation $Sh = 0.73(Re_{loc,r})^{0.25}(Re_t)^{0.32}(Sc)^{0.33}$ and the corresponding estimates derived *via* experimentally determined (◯) and theoretically predicted (g) velocity fields.

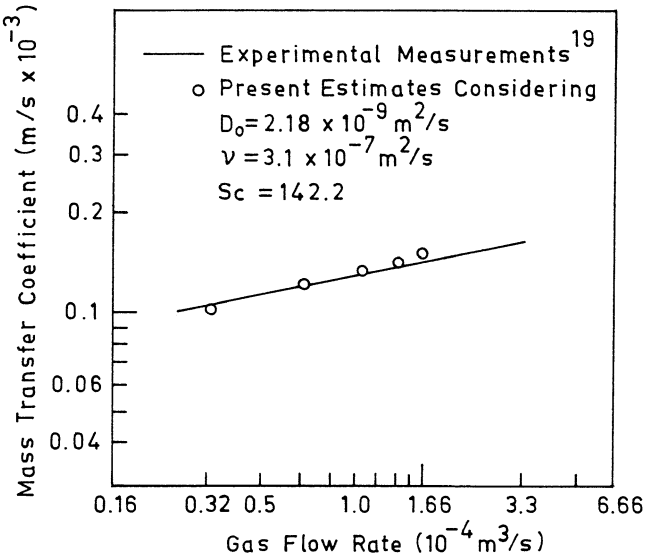

Fig. 7—Present estimates of mass transfer coefficients in a 25-kg gas-stirred Fe-C melt and their direct comparison with the corresponding experimental values reported by Wright.[19]

these together with the appropriate values for various thermophysical properties (*viz.*, $D_0 = 2.18 \times 10^{-9}$ m²/s, $\nu = 3.1 \times 10^{-7}$ m²/s, *etc.*) in the mass transfer correlation $Sh = 0.73(Re_{loc,r})^{0.25}(Re_t)^{0.32}(Sc)^{0.33}$, mass transfer coefficients $\left(K_{av} = \frac{Sh \cdot D_0}{d}\right)$ were predicted as a function of gas flow rates. Results thus obtained have been compared directly in Figure 7 with the corresponding experimental measurements in the 25-kg Fe-C melt, reported by Wright. Very reasonable agreement between predictions and measurements is readily apparent. On the basis of results presented so far, it is, therefore, reasonable to conclude that distributions of flow parameters $\overline{u}$, $\overline{v}$, $\hat{u}$, *etc.*, and hence various dimensionless groups $Re_{loc,r}$, Re_t, *etc.* in the system, the correlation $Sh = 0.73(Re_{loc,r})^{0.25}(Re_t)^{0.32}(Sc)^{0.33}$ is likely to provide reasonable estimates of solid-liquid mass transfer rates in gas bubble driven systems.

IV. CONCLUSIONS

A combined theoretical and experimental study on the dissolution of solid benzoic acid cylinders in an axisymmetric, gas-stirred bath has been carried out. Two different procedures were applied to obtain the mean and turbulence velocity fields in the system: (1) an experimental procedure based on LDV and (2) a theoretical calculation procedure based on the numerical solution of the turbulent Navier–Stokes equations. On the basis of these, nominal and turbulent Reynolds numbers (*viz.*, $Re_{loc,r}$ and Re_t) were estimated and embodied in the correlation $Sh = 0.73(Re_{loc,r})^{0.25}(Re_t)^{0.32}(Sc)^{0.33}$ to infer the corresponding mass transfer rates. Results obtained have demonstrated that both the procedures applied toward estimation of flow and

turbulence parameters are reasonably accurate and lead to realistic estimates of dissolution rates in gas-stirred systems. The adequacy of the present approach has also been assessed against experimental data reported in the literature on high-temperature dissolution, and reasonably good agreement between prediction and measurements has been demonstrated.

LIST OF SYMBOLS

A	surface area of the cylindrical compacts, m^2
C_s^*	saturation concentration limit of benzoic acid in water, kg/m^3
C_b	bulk concentration of benzoic acid in water, kg/m^3
d	diameter of solid samples, m
D	diameter of the vessel, m
D_0	diffusion coefficient, m^2/s
K_{av}	average mass transfer coefficient at any location, m/s
k	turbulence kinetic energy, m^2/s^2
L	depth of liquid in the vessel, m
M	mass of the cylindrical compacts, kg
R	instantaneous radius of the cylindrical compacts, m
R_i	initial radius of the cylindrical compacts, m
$\mathrm{Re}_{\mathrm{loc},r}$	local nominal Reynolds number $\left(\frac{d\rho\sqrt{u^2 + v^2}}{\mu}\right)$
Re_t	local turbulent Reynolds number $\left(\frac{d\rho\hat{u}}{\mu}\right)$
Sc	Schmidt number (ν/D)
Sh	Sherwood number ($K_{av}d/D_0$)
t	time, s
Tu	turbulence intensity[3] $\left(\frac{\sqrt{u'^2_{\mathrm{loc}}}}{\overline{u}_0}\right)$ ($\overline{u}_0$ = maximum centerline velocity, m/s)
u	axial mean velocity component, m/s
u'	RMS of the axial fluctuating velocity component, m/s
$\hat{u}$	isotropic fluctuating velocity component, m/s
v	radial mean velocity component, m/s
v'	RMS of the radial fluctuating velocity component, m/s
ρ_s	density of benzoic acid, kg/m^3
μ	viscosity of the bulk aqueous phase, kg/ms
ε	rate of turbulence kinetic energy dissipation, m^2/s^3
ν	kinematic viscosity of liquid (ρ/μ), m^2/s

REFERENCES

1. J. Szekely, T. Lehner, and C.W. Chang: *Ironmaking and Steelmaking*, 1979, vol. 6, pp. 285-93.
2. S. Taniguchi, M. Ohmi, S. Ishiura, and S. Yamauchi: *Trans. Iron Steel Inst. Jpn.*, 1983, vol. 23, pp. 565-70.
3. J. Szekely, J.H. Grevet, and N. El-Kaddah: *Int. J. Heat Mass Transfer*, 1984, vol. 27, pp. 1116-21.
4. D. Mazumdar, S.K. Kajani, and A. Ghosh: *Steel Res.*, 1990, vol. 61, pp. 339-46.
5. W.J. Lavender and D.C.T. Pei: *Int. J. Heat Mass Transfer*, 1967, vol. 10, pp. 529-39.
6. S. Whitaker: *J. AIChE*, 1972, vol. 18, pp. 361-71.
7. S. Asai, M. Kawachi, and I. Muchi: *SCANINJECT III*, 1983, pp. 11.1-11.30.
8. S.C. Koria: *Steel Res.*, 1988, vol. 59, pp. 484-91.
9. W.E. Ranz and W.R. Marshall: *Chem. Eng. Progr.*, 1952, vol. 48, pp. 141-46.
10. J.H. Grevet, J. Szekely, and N. El-Kaddah: *Int. J. Heat Mass Transfer*, 1982, vol. 25, pp. 487-96.
11. D. Mazumdar, R.I.L. Guthrie, and Y. Sahai: *Appl. Math. Model.*, 1993, vol. 17, pp. 255-62.
12. Y. Sheng and G.A. Irons: *Metall. Trans. B*, 1993, vol. 24B, pp. 695-705.
13. D. Mazumdar and R.I.L. Guthrie: *Metall. Trans. B*, 1985, vol. 16B, pp. 83-90.
14. D. Mazumdar: *Metall. Trans. B*, 1989, vol. 20B, pp. 967-69.
15. Y. Sahai and R.I.L. Guthrie: *Metall. Trans. B*, 1982, vol. 13B, pp. 203-11.
16. D. Mazumdar and R.I.L. Guthrie: *Iron Steel Inst. Jpn. Int.*, 1994, vol. 34, pp. 384-92.
17. B.E. Launder and D.B. Spalding: *Computer Meth. Appl. Mech. Eng.*, 1974, vol. 3, pp. 269-89.
18. S.T. Johanson and F.B. Boysan: *Metall. Trans. B*, 1988, vol. 19B, pp. 755-64.
19. J.K. Wright: *Metall. Trans. B*, 1989, vol. 20B, pp. 363-73.
20. A. Moult, D.B. Spalding, and N.C.G. Markatos: *Trans. Inst. Chem. Eng.*, 1979, vol. 59, pp. 200-04.